Modeling and Tracking Control of a Hydrostatic Dynamometer

Yu Wang, Zongxuan Sun, and Kim Stelson

Abstract— Traditionally automotive powertrain research and development have been conducted with electromagnetic dynamometers. The ever increasing demand for reducing fuel consumption and emissions has driven the innovation of new technologies in engines, transmissions, and hybrid systems, which in turn requires significant flexibilities and transient capabilities of the dynamometer. Given its superior power density, hydrostatic dynamometer is an ideal candidate for the next generation transient dynamometers. This paper presents the design, modeling, and control of a hydrostatic dynamometer as a precise torque device that could control the amount of torque supplied in real-time under both steady state and transient operations. The mathematical models are constructed for the system. Based on the analysis and simulation of the dynamic model, the dynamometer is decoupled into two subsystems. For the power output control subsystem, a nonlinear tracking controller based on feedback linearization and internal model principle is designed; for the operating pressure control subsystem, a PID regulator is designed. Simulation results in AMESim environment demonstrate the fast dynamic response and precise tracking capability of the proposed control system.

I. INTRODUCTION

Dynamometers have long been used to test automotive powertrain systems by emulating the loading conditions that may be experienced in real operations [1]. In other words, the function of a dynamometer is to "absorb" (or "provide", if necessary) the torque from (or to) the engine so that it is able to track the desired rotational speed and acceleration profile and, further, to provide the desired torque-speed conditions for fuel efficiency and emission testing. Given its superior power density, low inertia, and high bandwidth, hydrostatic dynamometer is an ideal candidate for the next generation transient dynamometers [2].

Some studies on hydrostatic dynamometers have been reported previously. Reference [3] presented a hydrostatic dynamometer consisting of a primary flow compensation pump/motor and a secondary torque absorbing pump/motor. Given a constant pressure drop, the dynamometer's torque was controlled by modulating the displacement of the secondary pump/motor [4]. Another dynamometer system was designed in [5]. Its principal components were a variable displacement unit controlling the displacement of the pump/motor, and a relief valve controlling the outlet pressure. Recently, a new hydrostatic dynamometer for single-cylinder engine testing was designed in [6]. Different from the previous

ones, it separated the system into a motor circuit and a pump circuit to generate the high/low inlet pressure corresponding to the motoring/absorbing torque conditions respectively, so as to optimize the power efficiency and dynamic response. With a high-bandwidth servovalve, the dynamometer had enough transient capability to make the single-cylinder engine produce the identical instantaneous speed trajectory as the multi-cylinder engine, and to take transient speed and load testing. The feedforward and PI/PD control strategies were utilized to produce the required dynamometer torque [7].

Our long-term research objective is to build a rapid prototyping hybrid powertrain testing and control platform using a transient engine dynamometer. Motivated by its high power density, a hydrostatic dynamometer with a load sensing mechanism is designed in this paper. Load sensing is essentially a self-feedback loop with the load pressure as the feedback signal, which ensures that the boost pump always provides the right amount of flow needed by the load. By means of the load sensing control, together with the nonlinear tracking controller, the dynamometer is able to manipulate all three main variables (inlet pressure, outlet pressure and pump/motor displacement) to control the torque. On this basis, the dynamometer can be used as a virtual power source or loading unit to emulate the torque-speed profile of any kind of hybrid power source (e.g. electrical motor or generator), and to test the various architectures and control strategies for the hybrid powertrain system.

However, to achieve precise speed profile tracking for the dynamometer is very challenging, since the hydraulic system is a highly nonlinear multivariable system, which cannot be easily modeled by a linear approximation. In addition, the system variables (torque, pressure, speed and flow rate) are coupled, and therefore a simple reduction in their dynamic interactions is not feasible. The challenges have attracted some research efforts on the control issues, related to both the hydrostatic and electrical dynamometers [8]-[9].

In order to overcome the challenges of the nonlinear dynamics, this paper presents a control strategy based on feedback linearization and internal model principle. The mathematical dynamic model is constructed and analyzed at first. On this basis, the dynamometer system is decoupled into the operating pressure control subsystem and the power output control subsystem. For the former subsystem, a PID regulator is designed to achieve the operating (inlet) pressure regulation; while, for the latter subsystem, since the fast and precise reference tracking is the primary control objective, feedback linearization is adopted to offset the nonlinearity of the system, and an internal-model based controller is designed to achieve

Yu Wang (e-mail: wang0930@umn.edu), Zongxuan Sun (corresponding author, phone: 612-625-2107; fax: 612-625-6069; e-mail: zsun@umn.edu) and Kim Stelson (e-mail: kstelson@me.umn. edu) are with the Department of Mechanical Engineering, University of Minnesota, Twin Cities, MN 55455 USA.

the reference tracking. Finally, simulation results in AMESim environment show the tracking performance.

II. SYSTEM MODELING

A. System architecture

The architecture of the hydrostatic dynamometer is shown in Fig.1and Fig.2 respectively.
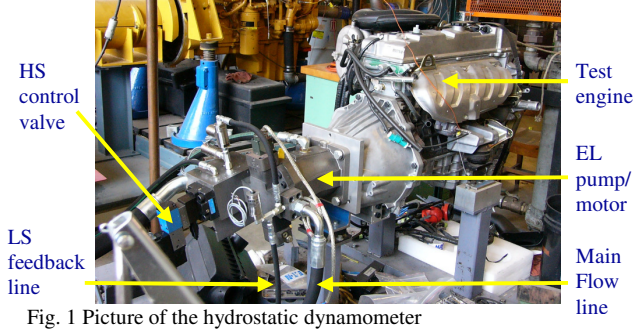

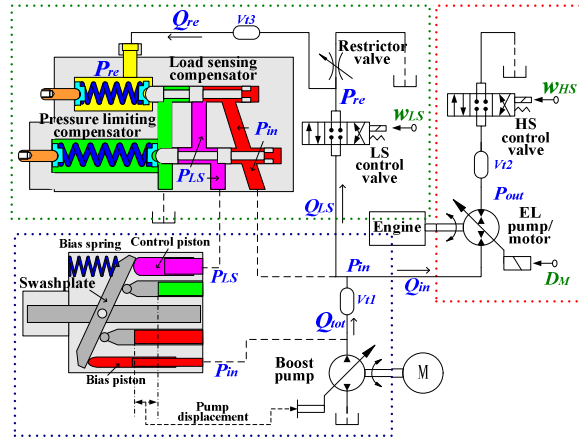Fig. 1 Picture of the hydrostatic dynamometer

Fig. 2 Architecture of the hydrostatic dynamometer

As shown in Fig.2, the boost pump and the engine load pump/motor (EL pump/motor) are both variable displacement piston pumps, and the load sensing control valve (LS control valve) and the high speed control valve (HS control valve) are both proportional valves. The load sensing and pressure limiting compensators, and the swashplate are all the internal configuration of the boost pump. Driven by an electrical motor, the boost pump provides the flow to the EL pump/motor. With the aid of the two control valves, the EL pump/motor is able to adjust the torque provided to the engine, and further, control either the steady state or the transient rotational speed of the engine.

Based on their intended functions, the dynamometer system in Fig. 2 is divided into three parts.

The load sensing and pressure limiting compensation part (in the green dashed line) is used to produce the proper outlet pressures P_{LS} of the load sensing compensator, so as to indirectly control the displacement of the boost pump.

The pump displacement adjustment part (in the blue dashed line) adjusts the swashplate angle, and hence, the displacement of the boost pump, by controlling the

displacements of the two pistons using the system operating pressure P_{in} and the load sensing outlet pressure P_{LS}.

The power output control part (in the red dashed line) controls the rotational speed and acceleration of the engine by manipulating the dynamometer torque. The torque is determined by the EL pump/motor displacement D_M and the pressure drop. If the operating pressure P_{in}, which is also the inlet pressure of the EL pump/motor, has been determined by the LS control valve, the outlet pressure P_{out} and the displacement D_M will be the only variables controlling the dynamometer torque.

B. Dynamic model

Based on the dynamometer architecture, as well as the fact that the operating (inlet) pressure can be measured by the sensors, we consider the inlet pressure as a time-varying parameter for the power output control part, so that the dynamometer torque is controlled specially by the commands to the HS control valve and EL pump/motor. This control strategy will decouple the dynamometer into two subsystems: the operating pressure control subsystem (including the load sensing and pressure limiting compensation part and the pump displacement adjustment part) and the power output control subsystem, as shown in Fig.3. The former only regulates the inlet pressure P_{in}; while the latter controls the outlet pressure P_{out} and, further, tracks the desired engine rotational speed, with the inlet pressure P_{in} as a time-varying parameter.
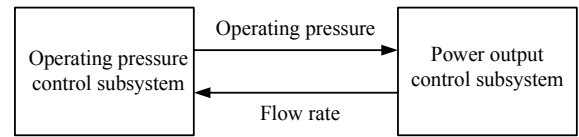

Fig. 3 Schematic diagram of the decoupled systems

1) Dynamic model of the power output control subsystem

The power output control subsystem consists of the EL pump/motor, the HS control valve and the tested engine.

The engine-dynamometer torque-speed dynamics is given by:

$$J\dot{\omega} = T_{engine} - T_{dyno} \qquad (1)$$

where ω is the engine rotational angular speed, rad/sec, J is the total moment of inertia of the engine and the EL pump/motor, T_{engine} is the engine torque output, and T_{dyno} is the dynamometer torque input, which is defined as:

$$T_{dyno} = \frac{D_m}{2\pi}\left(P_{out} - P_{in}(t)\right) \qquad (2)$$

where D_m is the displacement of the EL pump/motor.

The flow-pressure dynamics of the HS control valve is:

$$\frac{V_{t2}}{\beta_e}\dot{P}_{out} = Q_m - 2C_d A_{HS} w_{HS}\sqrt{\frac{2}{\rho}\left(P_{out} - P_0\right)} \qquad (3)$$

where V_{t2} is the volume between the EL pump/motor and the

HS control valve, β_e is the effective bulk modulus, C_d is the discharge coefficient, A_{HS} is the maximum orifice area of the HS control valve, w_{HS} is the open area ratio of the HS control valve, i.e., the ratio of the open orifice area and the maximum orifice area, ρ is the mass density of the fluid, P_0 is the outlet pressure of the HS control valve (almost 0 bar), Q_m is the flow rate passing through the EL pump/motor, defined as:

$$Q_m = \frac{D_m}{2\pi}\omega \tag{4}$$

We choose ω and P_{out} as the states, x_1 and x_2 , and w_{HS} and D_m as the inputs, u_1 and u_2 . The dynamics associated with the power output control subsystem is modeled as:

$$\begin{aligned}\dot{x}_1 &= -\frac{1}{2\pi J}x_2 u_2 + \frac{P_{in}(t)}{2\pi J}u_2 + \frac{T_{engine}}{J} \\ \dot{x}_2 &= \frac{\beta_e}{2\pi V_{t2}}x_1 u_2 - \frac{\beta_e R_{HS}}{V_{t2}}\sqrt{x_2}u_1\end{aligned}, \qquad y = x_1 \tag{5}$$

where $R_{HS} = 2C_d A_{HS}\sqrt{\dfrac{2}{\rho}}$ $\qquad(6)$

2) Dynamic model of the operating pressure control subsystem

The operating pressure control subsystem consists of the boost pump (including the internal compensators and swashplate) and the LS control valve.

The flow -operating pressure dynamics is given by:

$$\dot{P}_{in} = \frac{\beta_e}{V_{t1}}n_P D_P - \frac{\beta_e}{V_{t1}}R_{LS}w_{LS}\sqrt{P_{in}-P_{Re}} - \frac{\beta_e}{V_{t1}}Q_m \tag{7}$$

$$R_{LS} = 2C_d A_{LS}\sqrt{\frac{2}{\rho}} \tag{8}$$

where V_{t1} is the volume between the boost pump and the EL pump/motor, n_P is the rotational speed of the electric motor, w_{LS} , A_{LS} , P_{Re} and R_{LS} are the open area ratio, maximum orifice area, outlet pressure and resistance coefficient of the LS control valve respectively.
The flow-pressure dynamics of the LS control valve is:

$$\dot{P}_{Re} = \frac{\beta_e}{V_{t3}}R_{LS}w_{LS}\sqrt{P_{in}-P_{Re}} - \frac{\beta_e}{V_{t3}}R_{Re}w_{Re}\sqrt{P_{Re}} - \frac{\beta_e}{V_{t3}}Q_{FB} \tag{9}$$

where R_{Re} is the resistance coefficient of the restrictor valve, w_{Re} is the open area ratio of the restrictor valve, V_{t3} is the volume of the load sensing feedback pipe, Q_{FB} is the flow rate in the load sensing feedback pipe.

Furthermore, the LS compensator spool dynamics is:

$$\ddot{L}_x = -\frac{1}{m_c}f_c\dot{L}_x - \frac{k_c}{m_c}L_x + (P_{in}-P_{Re})\frac{S_c}{m_c} \tag{10}$$

$$Q_{FB} = -\dot{L}_x S_c \tag{11}$$

where L_x is the spool displacement of the LS compensator. At the initial position, L_x is zero when the main port (shown in purple in Fig. 2) is fully open to the left chamber (shown in

green in Fig. 2). m_c , f_c , k_c and S_c are the mass, the viscous friction coefficient, the spring rate and the chamber's cross sectional area of the LS compensator, respectively.

Besides the spool dynamics, the flow-pressure dynamics of the LS compensator are given as follows: When the main port is connected to the right chamber (shown in red in Fig. 2), i.e. L_x is larger than the port width L_{or} , there exists:

$$\dot{P}_{LS} = \frac{\beta_e C_d A_c \dfrac{L_x - L_{or}}{L_{or}}\sqrt{\dfrac{2}{\rho}(P_{in}-P_{LS})} - \beta_e S_{p-control}\dot{L}_y}{L_y S_{p-control} + V_{p0}} \tag{12}$$

Or, when L_x is smaller than the port width L_{or} , there exists:

$$\dot{P}_{LS} = \frac{\beta_e C_d A_c \dfrac{L_x - L_{or}}{L_{or}}\sqrt{\dfrac{2}{\rho}P_{LS}} - \beta_e S_{p-control}\dot{L}_y}{L_y S_{p-control} + V_{p0}} \tag{13}$$

where P_{LS} is the load sensing pressure, L_y is the displacement of the control piston from the left end, $S_{p-control}$ is the cross sectional area of the control piston, V_{p0} is the initial piston volume when L_y is zero, A_c is the maximum orifice area of the main port.

In addition, it is necessary to mention that the dynamics of the PL compensator are neglected, because it almost never affects the load sensing pressure P_{LS} , unless the operating pressure P_{in} exceeds the safety threshold.

Finally, the dynamics that relate to the displacement adjustment are analyzed. Based on the rotational motion of the swashplate, the dynamics is given by:

$$I_P\ddot{\theta} = -f_P\dot{\theta} + L_P\big[k_P L_P(\tan\theta_m - \tan\theta) - P_{LS}S_{P-control} + P_{in}S_{P-bias}\big] \tag{14}$$

where θ is the swashplate angle, θ_m is the maximum swashplate angle, L_P is the distance between the central axis of the control piston and pivot of the swashplate, I_p and f_P are the moment of inertia and the equivalent angular viscous friction coefficient of the swashplate respectively, k_P is the bias spring rate, S_{P-bias} is the cross sectional area of the bias piston.

Since θ is relatively small, we define that:

$$L_y = L_P(\tan\theta_m - \tan\theta) \approx L_P(\tan\theta_m - \theta) \tag{15}$$

Then, Eq. (14) can be converted into:

$$\ddot{L}_y = -\frac{f_P}{I_P}\dot{L}_y + \frac{L_P^2}{I_P}\big(-k_P L_y + P_{LS}S_{P-control} - P_{in}S_{P-bias}\big) \tag{16}$$

$$\frac{L_y}{L_p\tan\theta_m} = \frac{D_{P-max} - D_P}{D_{P-max}} \tag{17}$$

where D_{P-max} is the maximum boost pump displacement.

Eq.(7)-(17) are used to describe the dynamics associated with the operating pressure control subsystem.

Provided with the actual hardware parameters, the dynamometer model is constructed in AMESim, a

physics-based modeling and simulation software tool for hydraulic systems. The simulation results fully verify the validity of the system decoupling method and the dynamic models presented in this paper.

III. CONTROL DESIGN

A. Tracking control for the power output control subsystem

As introduced in the section II, the function of a dynamometer is to provide the proper torque input/output to "compensate" the engine torque, so as to drive the engine to track the desired rotational speed trajectory. Thus, essentially, the primary objective of the dynamometer control design is to enable fast and precise tracking for the reference speed.

Eq.(5) shows that the controller design is a MISO issue. However, the bandwidth of the EL pump/motor displacement adjustment is much lower than the HS control valve. Therefore, we prefer to use the HS control valve as the primary control actuator. However, as shown in Fig.4, if we use a constant EL pump/motor displacement, the dynamometer is either unable to cover the whole speed range due to the limited flow capacity of the HS control valve, or the outlet pressure may frequently exceed the safety threshold, especially with large dynamometer torque.
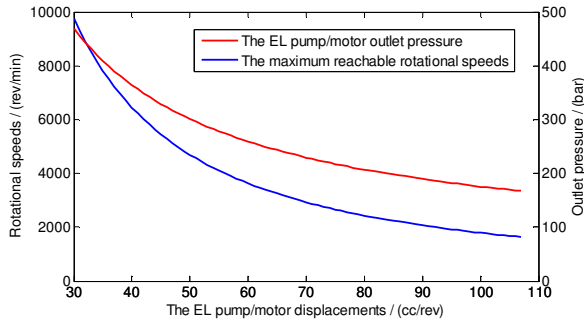

Fig.4 Maximum reachable rotational speeds and outlet pressures at different EL pump/motor displacements (where, the engine torque is 200 Nm and the inlet pressure is 50 bars)

Therefore, the SISO tracking controller based on the HS control valve control input is generated, and the displacement adjustment strategy for the EL pump/motor is designed, with the purpose of reducing the unnecessary high outlet pressure.

B. Tracking controller for the HS control valve

With the open area ratio of the HS control valve w_{HS} as the only input, as well as the EL pump/motor displacement as a time-varying parameter. The dynamic equations are given by:

$$\begin{aligned} \dot{x}_1 &= -\frac{D_m(t)}{2\pi J}x_2 + \frac{P_{in}(t)D_m(t)}{2\pi J} + \frac{T_{engine}}{J} \\ \dot{x}_2 &= \frac{\beta_e D_m(t)}{2\pi V_{t2}}x_1 - \frac{\beta_e R_{HS}}{V_{t2}}\sqrt{x_2}u \end{aligned}, \quad y = x_1 \quad (18)$$

1) Feedback linearization

Compared with the general Jacobian linearization, the feedback linearization, which is an exact representation of the original nonlinear model over a large set of operating

conditions, is more advantageous [10].

Feedback linearization is accomplished by subtracting the nonlinear terms out of the equations of motion and adding them to the control. At first, the nonlinear system in (18) will be rewritten in the form,

$$\dot{x} = f(x) + g(x)u, \qquad y = h(x) \quad (19)$$

where

$$f(x) = \begin{pmatrix} -\dfrac{D_m(t)}{2\pi J}x_2 + \dfrac{P_{in}(t)D_m(t)}{2\pi J} + \dfrac{T_{engine}}{J} \\ \dfrac{\beta_e D_m(t)}{2\pi V_{t2}}x_1 \end{pmatrix}, g(x) = \begin{pmatrix} 0 \\ -\dfrac{\beta_e R_{HS}}{V_{t2}}\sqrt{x_2} \end{pmatrix},$$

$$h(x) = x_1$$

$$(20)$$

Since that the system output is just the tracking object, the input-output feedback linearization is adopted. Considering the n th-order nonlinear system having relative degree $r = n$, the coordinates transformation required to construct the normal form is given exactly by:

$$\begin{aligned} \phi(x) &= \begin{pmatrix} \phi_1(x) & \phi_2(x) & \cdots & \phi_r(x) \end{pmatrix}^T \\ &= \begin{pmatrix} h(x) & L_f h(x) & \cdots & L_f^{r-1}h(x) \end{pmatrix}^T \end{aligned} \quad (21)$$

where the Lie algebra form is given by:

$$L_f h(x) = \begin{pmatrix} \dfrac{\partial h(x)}{\partial x_1} & \dfrac{\partial h(x)}{\partial x_2} & \cdots & \dfrac{\partial h(x)}{\partial x_n} \end{pmatrix} f(x)$$

$$L_f^n h(x) = \begin{pmatrix} \dfrac{\partial L_f^{n-1}h(x)}{\partial x_1} & \dfrac{\partial L_f^{n-1}h(x)}{\partial x_2} & \cdots & \dfrac{\partial L_f^{n-1}h(x)}{\partial x_n} \end{pmatrix} f(x)$$

$$(22)$$

In the new coordinates, the new states are defined as:

$$\xi_i = \phi_i(x) = L_f^{i-1}h(x) \qquad 1 \le i \le r \quad (23)$$

Then, we can get the Byrnes-Isidori normal form as:

$$\begin{aligned} \xi_1 &= h(x) = x_1 \\ \xi_2 &= \dot{\xi}_1 = L_f h(x) = -\frac{D_m(t)}{2\pi J}x_2 + \frac{P_{in}(t)D_m(t)}{2\pi J} + \frac{T_{engine}}{J} \\ \dot{\xi}_2 &= -\frac{D_m(t)^2 \beta_e}{4\pi^2 J V_{t2}}x_1 + \frac{D_m(t)R_{HS}\beta_e}{2\pi J V_{t2}}\sqrt{x_2}u - \frac{\dot{D}_m(t)}{2\pi J}x_2 \\ &\quad + \frac{\dot{P}_{in}(t)}{2\pi J}D_m(t) + \frac{\dot{D}_m(t)}{2\pi J}P_{in}(t) \\ &= v \end{aligned} \quad (24)$$

where v is the transformed input; the variable $P_{in}(t)$ and states x_1, x_2 can be measured by the sensors.

Furthermore, based on the third equation concerned with $\dot{\xi}_2$ in (24), the state feedback control law is defined as:

$$u = \frac{v + \dfrac{D_m(t)^2 \beta_e}{4\pi^2 J V_{t2}}x_1 - \dfrac{\dot{P}_{in}(t)}{2\pi J}D_m(t) + \dfrac{\dot{D}_m(t)}{2\pi J}x_2 - \dfrac{\dot{D}_m(t)}{2\pi J}P_{in}(t)}{\dfrac{D_m(t)R_{HS}\beta_e}{2\pi J V_{t2}}\sqrt{x_2}} \quad (25)$$

Now the resulting linear closed-loop system by the coordinate transformation is governed by the equations:

$$\begin{aligned} \dot{\xi}_1 &= \xi_2 \\ \dot{\xi}_2 &= v \end{aligned}, \quad y = \xi_1 \quad (26)$$

2) Internal model-based controller

In linear time-invariant systems, reference tracking or disturbance rejection requires that the generating polynomial is included as part of the controller denominator. This is known as the Internal Model Principle (IMP).

In order to simplify the reference tracking issue, we assume that the reference signal, which is the desired rotational speed, is a function of the linear and quadratic signals, given by:

$$r(t) = K_0 + K_1 t + K_2 t^2 \qquad (27)$$

where K_0 - K_2 are constant. Then the generating polynomial is:

$$\Gamma_r(s) = s^3 \qquad (28)$$

where s is the complex variable in Laplace Transform.

For the linearized model (26), the nominal plant model is:

$$G_o(s) = \frac{B_o(s)}{A_o(s)} = \frac{1}{s^2} \qquad (29)$$

The internal model-based controller model is given by:

$$C(s) = \frac{P(s)}{\Gamma_r(s)\bar{L}(s)} \qquad (30)$$

Thus, the denominator of closed-loop feedback loop is:

$$A_{cl}(s) = \Gamma_r(s)\bar{L}(s)A_o(s) + P(s)B_o(s) \qquad (31)$$

where, $\bar{L}(s) = l_1 s + l_0$, $\quad P(s) = p_4 s^4 + p_3 s^3 + \cdots + p_0 \qquad (32)$

In order to ensure the stability of the closed-loop system, all the poles are placed at -10, i.e. $A_{cl}(s) = (s+10)^6$. Solve it and get l_0, l_1, p_0 - p_4, and the internal model-based controller is:

$$C_{IMP}(s) = \frac{p_4 s^4 + p_3 s^3 \cdots + p_0}{s^3(l_1 s + l_0)} \qquad (33)$$

The nonlinear tracking controller is shown in Fig. 5.

Nonlinear controller

Transformed linear system

r + err → IMP controller $C_{IMP}(s)$ → v → Feedback linearization $C_{ff}(s)$ → u → Plant Go(s) → y, x_1, x_2
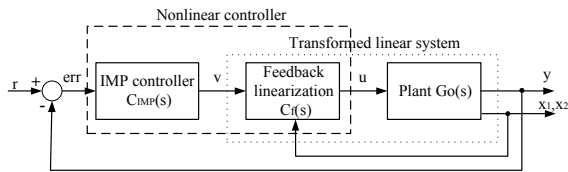
Fig.5 Schematic diagram of the nonlinear controller

C. Control strategy for the EL pump/motor displacement

Because of its high bandwidth, we prefer the HS control valve as the primary actuator. However, the reachable rotational speed using only the HS control valve is limited.

In the steady state, i.e., $\dot{x}_1 = \dot{x}_2 = 0$, the mathematic relationship of the system in (18) is given by:

$$-\frac{D_m^3}{8\pi^3 R_{HS}^2 J}\frac{x_1^2}{u^2} + \frac{P_{in}}{2\pi J}D_m + \frac{T_{engine}}{J} = 0 \qquad (34)$$

Given a displacement D_m, when the open area ratio of the HS control valve u is 100%, the maximum reachable speed is:

$$\omega_{max} = x_1 = u_{\bar{u}=100\%}\sqrt{\frac{8\pi^3 R_{HS}^2}{D_m^3}\left(\frac{P_{in}}{2\pi}D_m + T_{engine}\right)} \qquad (35)$$

The basic adjustment strategy for the EL pump/motor displacement is defined as follows: for a given operating displacement D_m, if the instantaneous rotational speed exceeds the threshold ω_{max}, then the EL pump/motor will be adjusted into a larger operating displacement; otherwise the current displacement will be maintained. Meanwhile, the controller based on the HS valve control input is always operating. Thus, the confliction between full-range speed tracking and outlet pressure limiting is removed.

To improve the tracking performance, some modifications in the adjustment strategy are taken in practice, as follows:

1) Choice of the operating displacements

In order to avoid frequent displacements adjustment that induces excessive transient oscillations, we choose only three points: $D_{m0} = 80 cc/rev$, $D_{m1} = 55 cc/rev$, $D_{m2} = 40 cc/rev$.

2) Calculation of the maximum reachable speed ω_{max}

Ideally, we should substitute $u = 100\%$ into (35) to get the maximum reachable speed ω_{max}. However, at this moment the tracking control of the HS control valve cannot work fully because the input u cannot rise any longer, which may induce the intense speed oscillations. In this case, we consider remaining the enough adjustable space for u when the displacement adjustment happens. Therefore, the maximum reachable speed ω_{max} will be defined with $u = 95\%$.

D. PID regulator for the operating pressure control subsystem

The operating pressure control subsystem is a highly-nonlinear high-order dynamic system, however, based on the beneficial self-feedback characteristic of the load sensing control mechanism, a PID regulator can be designed.

With the Ziegler-Nichols Tuning method, the proportional gain is increased gradually until the system becomes marginally stable and continuous oscillations just begin. At that time, the corresponding gain is defined as ultimate gain K_u, and the period of oscillation is defined as ultimate period P_u. Then, the PID regulator is designed by:

$$C(s) = K_P\left(1 + \frac{1}{T_I s} + T_D s\right) \qquad (36)$$

where, $K_P = 0.6K_u$, $\quad T_I = 0.5P_u$, $\quad T_D = 0.125P_u$

In simulation, the ultimate sensitivity parameters are tuned to be $K_u = 3\times10^{-6}$ and $P_u = 0.044\,sec$.

IV. SIMULATION RESULTS

The dynamometer dynamic model and controllers are structured in AMESim environment, with the model parameters shown in Table 1. The dynamometer simulation results for the rotational speed tracking are shown in Fig. 6-8.

Figure 6 shows the desired speed trajectory and tracking error. It is clear that, the nonlinear controller can achieve precise reference profile tracking, only with minor speed oscillations in the boundary area where the different EL pump/motor displacements are switched, or in the vicinity of

the time points when the speed changes abruptly. These oscillations are caused by the sharp charge of the plant model (the pump/motor displacement) or the reference signal. In most cases, the magnitude of the transient errors is less than 1.5% of the desired reference signal.

Fig.7 shows the inlet/outlet pressure. The PID regulator successfully achieves the inlet pressure regulation (50 bars), except when the speed changes abruptly. Figure 8 shows the control signals.

TABLE I
MAIN PARAMETERS IN THE SYSTEM DYNAMIC MODEL

| Symbol		Quantity
T_{engine}	engine torque	200 (N*m)
J	moment of inertia	0.15 (kg*m^2)
D_{pmax}	maximum boost pump displacement	131(cc/rev)
R_{HS}	HS valve coefficient	7.127*10^{-7}(m^3/sec/pa$^{1/2}$)
R_{LS}	LS valve coefficient	2.434*10^{-8}(m^3/sec/pa$^{1/2}$)
R_{Re}	Restrictor valve coefficient	8.607*10^{-9}(m^3/sec/pa$^{1/2}$)
V_{t1}	pipe volume	0.00069(m^3)
V_{t2}	pipe volume	0.001(m^3)
V_{t3}	pipe volume	0.000096(m^3)
n_P	electrical motor speed	2000(rpm)
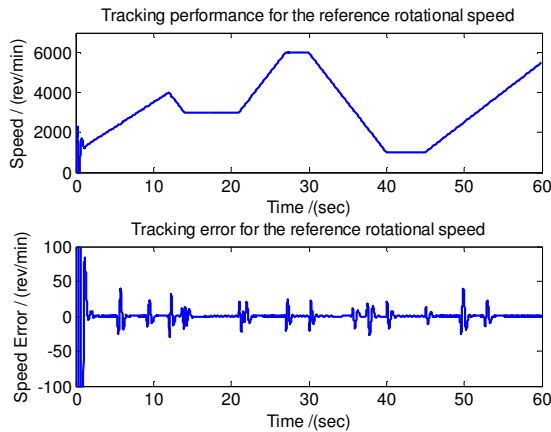
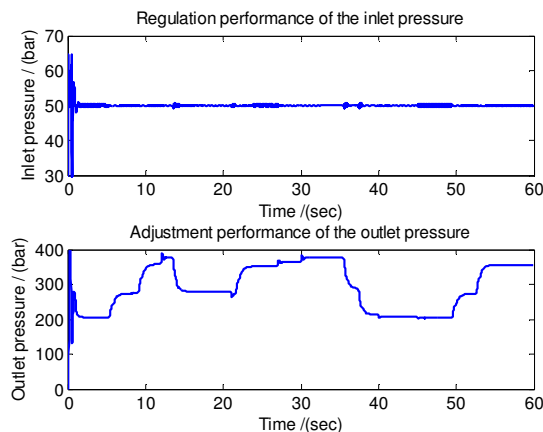Fig. 6 Desired speed trajectory and tracking error

Fig. 7 Regulated trajectory of the inlet/outlet pressure
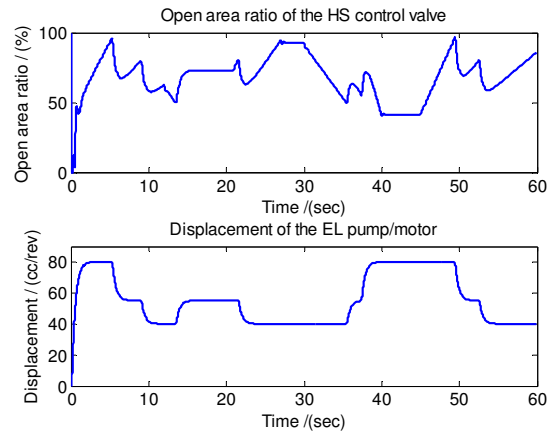

Fig. 8 Trajectory of the two control inputs

V. CONCLUSION

This paper presents the modeling and control of a transient hydrostatic dynamometer. A detailed dynamic model has been constructed. A nonlinear tracking controller based on feedback linearization and internal model principle and a PID regulator have been designed for the two dynamometer subsystems, respectively. The simulation results in AMESim environment have demonstrated that the controllers are capable of fast and precise tracking of the desired rotational speed.

REFERENCES

[1] B. J. Bunker, M. A. Franchek, B. E. Thomason. "Robust multivariable control of an engine-dynamometer system", *IEEE Transactions on Control Systems Technology*, 1997, 5(2), pp. 189-199

[2] G. R. Babbitt, J. J. Moskwa. "Implementation details and test results for a transient engine dynamometer and hardware in the loop vehicle model", *Proceedings of International Symposium on Computer Aided Control System Design*, Hawaii, 1999, pp. 569-574.

[3] Schenck Pegasus. "Automatic control behavior of driveline and loading machines for dynamic engine testing", *Schenck Pegasus Technical literature L3920 e*, Darmstadt, Germany.

[4] G. R. Babbitt. "Transient engine test system for hardware-in-the-loop powertrain development", *Ph.D. dissertation*, University of Wisconsin-Madison, 1999.

[5] H. Ghaffarzadeh, M. Guebeli, N. D. Vaughan. "Linear model identification of a hydrostatic dynamometer through dynamic simulation", *Proceedings of 5th Bath International Fluid Power Workshop*, University of Bath, UK, 1992, pp. 416-430.

[6] J. L. Lahti, J. J. Moskwa. "A transient hydrostatic dynamometer for testing single-cylinder prototypes of multi-cylinder engines", *2002 Society of Automobile Engineer Technical Paper*, Detroit, Michigan, 2002-01-0616.

[7] J. L. Lahti, J. J. Moskwa. "A transient test system for single cylinder research engines with real time simulation of multi-cylinder crankshaft and intake manifold dynamics", *2004 Society of Automobile Engineer Technical Paper*, Detroit, Michigan, 2004-01-0305.

[8] D. U. Campos-Delgado, D. R. Espinoza-Trejo, E. Palacios. "Closed-loop torque control of an absorbing dynamometer for a motor test-bed", *Proceedings of International Symposium on Industrial Electronics*, 2007, pp. 2113-2118.

[9] G. R. Babbitt, R. L. R. Bonomo, J. J. Moskwa. "Design of an integrated control and data acquisition system for a high-bandwidth, hydrostatic, transient engine dynamometer", *Proceedings of the American control conference*, Albuquerque, New Mexico, 1997, pp. 1157-1161.

[10] A. Isidori. *Nonlinear control system*. London, Inc. 1995, pp. 137-211.